Informes de la Construcción
Vol. 73, 564, e421
octubre-diciembre 2021
ISSN-L: 0020-0883
https://doi.org/10.3989/ic.84138

A protocol for using unmanned aerial vehicles to inspect agro-industrial buildings

Protocolo para el uso de vehículos aéreos no tripulados en la inspección de edificios agroindustriales

Javier Gómez (*), Alberto Tascón (**)

RESUMEN

Unmanned aerial vehicles, commonly known as drones, have many potential applications in the building industry. Among the most evident of these is inspection of buildings during construction and commissioning and as part of the maintenance strategy throughout service life. Drones can also be combined with thermal imaging for energy assessment of buildings. The present study describes an inspection protocol for agro-industrial buildings that consists of 5 stages, each composed of multiple tasks. The protocol was developed based on previous reports from other sectors, existing regulations and the authors' own experience. In addition, it was validated through application to a real case: a recently built wine-ageing facility measuring 7,200 m² with mechanical heating/cooling. The inspection yielded useful graphical information with both visible and infrared video and revealed difficulties, aspects to take into account and precautions to adopt in future use of these systems.

Palabras clave: Drone; building inspection; building envelope; thermography; winery.

ABSTRACT

Los vehículos aéreos no tripulados, comúnmente denominados drones, son una tecnología con muchas aplicaciones potenciales en la construcción. Entre las más evidentes está la inspección de edificios durante las fases de construcción y puesta en servicio o como parte de su programa de mantenimiento. Los drones también pueden combinarse con la termografía para realizar evaluaciones energéticas. Este trabajo presenta un protocolo para la inspección de edificios agroindustriales formado por 5 fases, cada una constituida por diversas tareas. El protocolo se desarrolló a partir de experiencias previas reportadas en otros sectores, regulaciones existentes y la propia experiencia de los autores. Además, se ha validado mediante su aplicación a un caso real: una nave climatizada para crianza de vino de 7.200 m² recién construida. La inspección proporcionó información gráfica de utilidad, tanto visible como infrarroja, y se detectaron dificultades, aspectos a considerar y precauciones para el uso de estas tecnologías.

Keywords*: Dron; inspección de edificios; envolvente; termografía; bodega.*

(*) PhD Agricultural Engineer. Senior Design Engineer. Faber 1900 Architecture & Engineering Studio, Logroño (Spain).
(**) PhD Agricultural Engineer. Associate Professor. University of La Rioja, Logroño (Spain).
Persona de contacto/*Corresponding author*: alberto.tascon@unirioja.es (A. Tascón)
ORCID: http://orcid.org/0000-0002-6691-0993 (J. Gómez); http://orcid.org/0000-0001-9379-2702 (A. Tascón)

Cómo citar este artículo/*Citation:* Javier Gómez, Alberto Tascón (2021). A protocol for using unmanned aerial vehicles to inspect agro-industrial buildings. *Informes de la Construcción,* 73(564): e421. https://doi.org/10.3989/ic.84138

Recibido/*Received*: 09/10/2020
Aceptado/*Accepted*: 15/04/2021
Publicado on-line/*Published on-line*: 24/11/2021

1. INTRODUCTION

The use of unmanned aerial vehicles (UAV), commonly known as drones, has spread widely and rapidly in the civil sector over the past few years. Use of UAVs is now common for a variety of applications, including precision agriculture, 3D mapping, infrastructure inspection, search and rescue missions, road traffic monitoring, and many others (1).

The building sector has started to explore the use of UAV technologies, for example in 3D building modelling (2), construction progress tracking (3), cultural heritage interventions (4), façade inspection (5) and health and safety management (6). However, several challenges remain as regards the adoption of drones in the construction sector (7). One serious limitation is the absence of standardised technical procedures, particularly for industrial buildings. Therefore, there is a need to develop methods to serve as guidance and help to advance the discussion on how to employ this technology.

Building inspections using drones could be carried out during execution and commissioning of the building or as part of a maintenance strategy throughout service life; in both cases, drones could be used in combination with thermal imaging cameras to conduct energy assessments (8). A priori, drones have the potential to obtain important information in less time, at a lower cost and with less risk to personnel compared with conventional inspection of buildings (9), especially with respect to high elements such as the upper part of walls, roofs, tanks and silos.

Infrared (IR) thermal imaging, also known as thermography, is a non-contact, non-destructive testing technology that converts the infrared radiation emitted from bodies into thermal images, showing surface temperature distribution. Currently, the principal use made of thermography in the construction sector is qualitative, to detect thermal anomalies based on simple observation of images that are usually obtained from inside the building (10). However, quantitative thermography can also be applied, for example, to the evaluation of building thermal transmittance (11). Detection of either moisture, hidden materials and structures, cracks, corrosion or microbial biofilms are other potential uses of IR images in buildings (12-14). Thermography and drones are not commonly used in combination in the construction sector, and it is therefore important to explore the use of IR-UAV systems in these early stages of utilization in order to maximise synergies between the two technologies.

The main goal of this study was to propose a protocol for using drones to inspect agro-industrial buildings. This research builds upon authors' prior work (15). In the present study, preliminary versions of the methodology have been modified and extended. Difficulties, aspects to take into account and precautions to adopt were also identified. In addition, the proposed protocol was tested and validated by means of a real-life inspection.

2. MATERIALS AND METHODS

2.1. Inspection protocol

The design of the inspection protocol was based on previous studies in other fields, existing regulations and the authors' practical experience (15). In particular, the method applied by Seo *et al.* (16) to inspect bridges in forestry areas and the thermographic analysis of buildings reported by Entrop and Vasenev (17) were taken as the base for this protocol. In addition, current regulations for safe drone operation in Spain were observed (18). Recommendations for correct application of thermography (10) were also considered, since an IR-UAV system was used in this study. This prior information was tailored to the specific case of agro-industrial buildings in order to develop a systematic method for efficient inspection of these constructions. The objective of the inspection would be twofold: first, to obtain visual information by means of an optical camera; and, second, to get infrared (IR) thermal data. The proposed protocol consists of 5 stages, as shown in Table 1.

Stage 1 consists of reviewing previously available information on the building to inspect in order to identify the elements and potentially critical locations to examine. Technical drawings, previous inspection reports and aerial images from applications such as Google Earth can all be used in this stage. The selection of the building elements to be inspected depends on the objectives and scope of the survey. If the aim were to assess the overall thermal performance of the building or to detect unexpected thermal anomalies, it would be advisable to inspect the entire envelope, including all walls, roofs, windows, doors, etc. However, in other cases, including assessments of insulation material degradation and partial retrofit interventions, it could be sufficient to inspect only those elements involved. Singular elements, i.e. geometrical thermal bridges and other elements that were less insulated than the rest, should be always identified prior to the inspection.

The aim of stage 2 is to identify potential risks such as trees, power lines, aerials, roads and other nearby buildings in order to define a safe drone flight. It will be necessary to conduct an on-site visit, if this has not already been done in stage 1, in order to correctly identify all risks. Consideration should also be given to drone pilot safety, especially if the drone must be operated from a location where vehicles circulate. Existing regulations and flight restrictions must also be considered during this stage: according to current Spanish regulations (18), it is obligatory to draw up an aviation safety report prior to the flight. Risk analysis and existing regulations will determine the areas for drone takeoff and landing, and for assembly and disassembly in the event that the drone is transported disassembled. The flight plan is also defined at this stage, including flight path and drone movements (horizontal, vertical and turns), horizontal and vertical distances to maintain from building elements and obstacles and camera angles and distances to maintain in relation to the elements to inspect. Stage 2 is also when the most suitable drone and sensors are selected according to the task to perform and the risks identified. Drones can be equipped with different types of sensor, depending on the purpose of the flight (1). Some drones have integrated cameras and IR sensors, and others not. The total inspection time and the number of batteries required should be estimated in Stage 2 to plan the interval stops and the different phases of the flight inspection.

Stage 3 consists of drone inspection and preparation. A detailed pre-flight inspection is recommended, revising all elements (e.g. batteries, rotors, sensors and cameras, remote control, GPS system). This is also the stage when the thermal imaging camera must be calibrated, setting level and span

(10). The level refers to the maximum and minimum temperatures that define the extremes of the temperature span, and should always be adapted to the temperature range of interest. The span determines the contrast of thermal images and should be neither too high nor too low. In addition, the colour palette must be selected, with rainbow palettes being the most frequently used.

Table 1. Protocol for agro-industrial building inspection

Stages and tasks to perform
1. Collection of prior information on the building
a. Study of drawings and location
b. Identification of building envelopes to inspect
c. Identification of critical points and details to inspect
2. Study of operational safety and flight plan
a. Identification of potential risks
b. Selection of pilot position(s)
c. Selection of area(s) for takeoff and landing
d. Definition of flight plan
e. Selection of the most suitable drone and instrumentation
f. Consultation of weather forecast and selection of days and times
3. Inspection and calibration of the drone and its accessories
a. Inspection of drone components and battery charging
b. Drone assembly
c. Inspection and calibration of cameras and GPS
d. Control unit and connectivity testing
4. Execution of flight
a. Annotation of day, time and weather conditions
b. Execution of previously defined flight plan
c. Verification of information obtained by the drone
5. Analysis of information
a. Identification of deficiencies in the envelope
b. Identification of thermal anomalies
c. Preparation of report of results

Stage 4 comprises building inspection by the drone, following the previously defined flight plan and the aviation safety report.

Lastly, stage 5 includes a study and analysis of the information collected by the drone, identifying envelope deficiencies and thermal anomalies, if any. The final step is to draw up a report of the results for submission to the client.

2.2. Drone description

A DJI Mavic 2 Enterprise DUAL drone was used for the present study. This model is a quadricopter weighing 0.9 kg. It is equipped with an optical camera capable of capturing 12-megapixel images and recording 4K Ultra HD videos (3840×2160), and a FLIR Lepton thermal micro-camera for the long-wave (LW) region (from 8 to 14 μm) with the following specifications: 120 x 160 resolution, 57° visual field, range of -10° to 140°, accuracy of ±5%.

The selected drone is shown in Figure 1. It is small, facilitating handling and transport in any vehicle, and is equipped with an efficient stabiliser to ensure the stability and quality of images. It has a battery life of approximately 30 minutes in standard favourable flight conditions. The drone is operated by a remote controller with a 5.5-inch built-in screen, which together with the accompanying DJI app displays real-time images captured by the optical and IR cameras. This drone was selected on the basis of its low cost and its good performance and versatility in relation to the intended use. The goal was to select a user-friendly drone, given its intended use as an inspection tool for by a wide variety of professionals. Seo et al. (16) conducted a comparison of drones based on a series of criteria, which should be selected and adapted according to the particular intended use of the drone. However, it should be noted that UAV technologies are evolving rapidly and therefore it is likely that drone capacities and costs will also change rapidly in the coming years.

Figure 1. Drone employed to validate the inspection protocol.

The coloured images that are obtained with the IR drone camera represent the apparent temperatures of the different target objects. These apparent temperatures are calculated from the thermal radiation emitted by the objects and recorded by the IR sensor, which in turns mainly depends on the real temperature of the objects, the emissivity factors of the materials and the orientation of the camera in relation to the objects (10). Thus, not all differences detected by the camera imply differences in the real temperatures of the objects. A critical examination of the thermal pictures and videos is required, along with expertise in this technique.

2.3. Agro-industrial building description

The building selected was a recently constructed wine-ageing facility that was still in the commissioning stage (Figure 2). It belonged to a winery producing Rioja wine (19). The winery was surrounded by vineyards and had several other buildings of varying ages for different purposes.

Since the building was very large (approximately 7,200 m^2 and 65,000 m^3), it was of interest to use a UAV to verify that the construction work had been carried out appropriately and that the building envelope did not present defects. In addition, wine-ageing requires specific thermal conditions (20), and therefore buildings intended for this purpose are usually equipped with a heating/cooling system which entails significant energy expenditure; consequently, it was of interest to conduct a thermographic study. In this case, the building

had a heating/cooling system that maintained the internal temperature at 15-17°C at all times. The building housed a large space devoted to wine ageing in barrels, a tasting room, a barrel washing room and some wine storage tanks; the other operations of the winemaking process (21), including the receipt and crushing of the grapes, fermentations, bottling, ageing in bottles, etc., were carried out in other buildings of the same winery.

Figure 2. Aerial image of the selected building, captured by the drone.

The building measured 120.43 m long, 60.43 m wide and 9.13 m high to the eaves. All process areas and storage rooms were above ground, and the building also had two mezzanine areas. The upper envelope consisted of 5 identical hipped roofs made of ceramic tiles resting on metal battens and 120 mm-thick ribbed sandwich panels. The panels were composed of rock wool insulation sandwiched between metal sheeting with an imitation wood finish in the internal side. The walls consisted of precast reinforced concrete panels with a core made of insulation material. In the interior, these had an air chamber and 11.5 cm-thick face brick cladding. The exterior side of the panels was lined with 10 cm-thick rock wool insulation, an air chamber and 11.5 cm-thick face brick cladding. The building had several access doors for vehicles and people, all fitted in metal frames with copper sheeting and rock wool insulation. It also had several triple glazed windows on the southwest and northwest faces. In addition, the building had a flue for the ventilation of the barrel washing room, where barrels are cleaned with steam, and another for the boiler combustion chamber (number 17 in Figure 3). The building also had a heating, ventilation and air-conditioning system (HVAC unit) to control indoor environment, several ventilation grilles for air intake for the HVAC unit and the boiler (numbers 16 and 18 in Figure 3), and a large chimney for exhaust air from the ventilation system (number 15 in Figure 3).

2.4. Application of inspection protocol to the selected building

Inspection of the building was carried out following the 5 stages of the proposed protocol. Some aspects of interest are described below.

During stage 1, the building dimensions and the characteristics of its envelope, which are summarised in the above section, were gathered. Also, information on the location of the building and others nearby was collected. Then, a sketch was drawn identifying elements such as access doors, windows and trees with a view to planning the inspection (Figure 3). Numbering the elements facilitated the flight and subsequent systematic and efficient analysis of results.

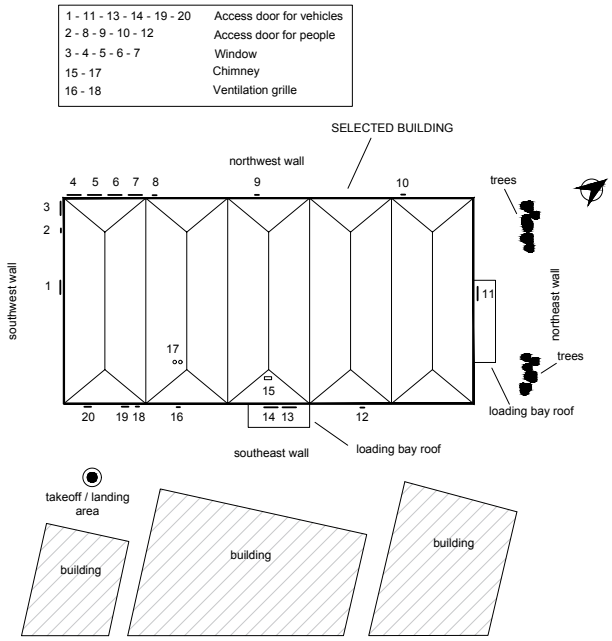

Figure 3. Building element numbering in plan view.

In stage 2, the potential risks associated with the drone flight were analysed. In this case, this was a free-standing building located within the winery grounds and therefore the risks were minimal. The only obstacles that could have posed a risk were several large trees located at some distance from the northeast face of the building and two exterior loading bays at the northeast and southeast walls, both of which had a permanent tiled roof supported by several concrete columns (Figure 3). However, there was enough free space to allow the drone to pass safely between the trees and the building or between the trees and the roof of the northeast loading bay. In addition, the entire perimeter of the building was paved, enabling the pilot to physically accompany the drone during inspection of the walls. Signage was placed to prevent vehicles from entering the takeoff/landing area and the pilot's various locations along the building walls throughout the duration of the flight. To increase operational safety, the pilot was accompanied at all times by an assistant who was responsible for preventing the passage of vehicles. The other three buildings located at some distance from the southeast wall were part of the same winery.

The drone flight path was designed based on the information collected previously. It was decided to control the flight manually, using the remote controller screen and, where possible, maintaining eye contact with the drone. Thus, the GPS guiding system was not used. It was also decided to collect data by means of video rather than via photography, since 3D photogrammetry and subsequent CAD modelling did not fall within the scope of the inspection objectives. Therefore, a video (visible and infrared images) was recorded continuously during inspection, but no photograph sequences were taken at predetermined points, greatly simplifying flight plan design and execution.

Exterior walls and roof required two distinct approaches and types of flight. For the walls, a flight was designed in which the drone moved horizontally along the building perimeter, maintaining a distance of approximately 10 m from the same.

For the roof, the flight was designed as a series of horizontal zigzag bands, with the drone flying at an altitude of about 20 m above the highest point of the building (37 m above ground level). The characteristics of both flight paths are shown in Figures 4 and 5.

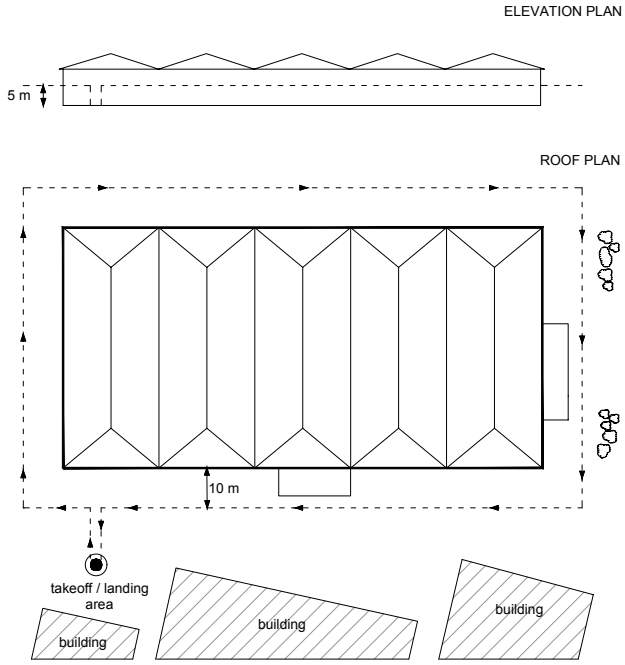

Figure 4. Flight paths for walls inspection.

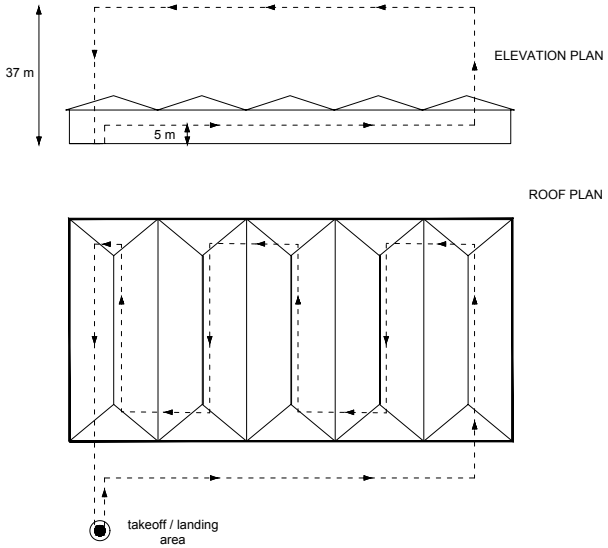

Figure 5. Flight paths for roof inspection.

Only days when rain, storms or fog were not forecast were selected for flying. Duplicate flights were planned: a first flight at mid-day in order to obtain a video with visible light and a second flight at dawn – before sunrise and with temperature ≤ 5°C – to record an infrared thermal imaging video.

During stage 3, it was checked if either the DJI pilot app or the status indicator requested compass calibration (this was not the case), and the remote controller connectivity was tested. Prior to the thermal inspection flight, IR camera settings were selected by measuring the temperature at 3 points on the building envelope and then adding 7 °C above and below the mean value; the total span was thus set at 14°C (10).

Execution of the building inspection with the drone corresponded to stage 4. Inspection flights were executed under favourable weather conditions, without rain and with good visibility and wind speeds below 20 km/h. Two batteries were necessary to execute one single inspection, which included one flight to inspect the walls and another one for the roof. These two flights lasted about 35 minutes plus 10 minutes for drone assembly/disassembly and checking. As mentioned above, the inspection flights were duplicated, so the total time was approximately 90 minutes. The last stage of the inspection protocol (stage 5) consisted of downloading and analysing the data obtained by the drone.

3. RESULTS

The inspection flights provided videos of both visible and thermal images covering the entire building envelope. These videos were used for confirming correct execution of the construction work. The amount of data generated during this study was approximately 50 Gb for the visible images and 780 Mb for the IR images. Figure 6 shows one image of the building envelope extracted from the video taken by the drone during the first inspection flight. Similarly, Figures 7, 8, 9 and 10 collect several IR images recorded by the drone during the second inspection flight; in all these figures camera level and span are shown at the bottom. As illustrated in Figures 8, 9 and 10, the drone's thermal camera detected temperature differences in some envelope elements. These differences were analysed to ensure that they were not due to faulty insulation installation or any other construction error, by following the general principles for qualitative thermographic examination in standards and handbooks (10, 22). However, it is important to remark that thermal images interpretation involves a high level of subjectivity and mainly relies on the expertise of the human operator, as pointed out by Garrido *et al.* (23). For that reason, some research has aimed at developing methods for automatic detection and characterisation of thermal bridges (23, 24).

Figure 6. Image of the building envelope taken by the drone during the first inspection flight.

4. DISCUSSION

The inspection revealed that the building envelope had been correctly executed and that insulation uniformity was excel-

lent in walls and roofs alike. For example, Figure 7 illustrates the absence of thermal anomalies in the building roof. The drone's thermal camera detected some temperature differences where this was to be expected, i.e. elements that were less insulated than the rest, such as windows and doors (Figure 8). Also, the flue that extracted air from the barrel washing room, whose temperature was much higher than the outdoor air temperature, was clearly identified (Figure 9).

Figure 10 shows that the underside of the eaves and the upper region of the side walls were warmer than the lower part of the walls; this can also be seen in Figure 8. This phenomenon can be explained by the effect of the roof overhang on the clear sky radiant cooling rate (10): the warmer elements had sustained less radiative losses during the night because of their angles to the zenith, 180º and 90º, respectively.

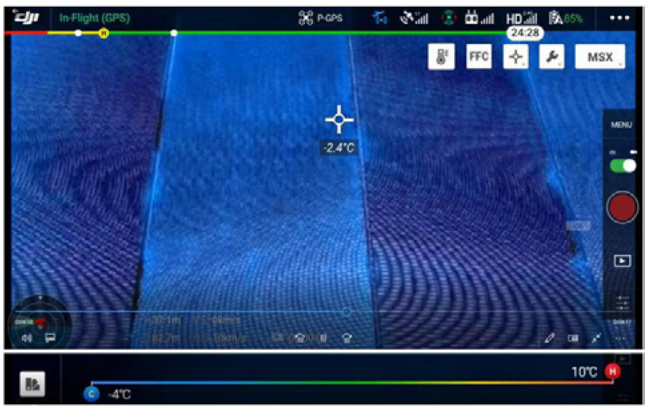

Figure 7. Thermal image of the roof taken by the drone.

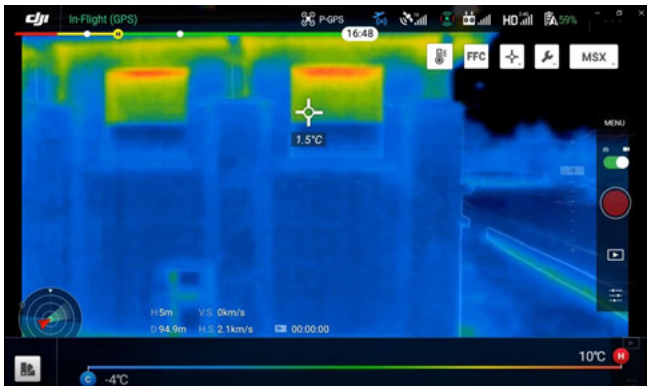

Figure 8. Temperature differences detected by the thermal camera: Windows and door.

Vollmer and Möllmann (10) demonstrated that clear night sky radiant cooling can generate a difference of 8°C between horizontal surfaces covered with aluminium foil – which reduces radiative losses – and uncovered surfaces facing the sky, or a difference of 6°C in the case of vertical wall surfaces. They even detected an area on part of a wooden house wall below a carport roof that was 3°C warmer than unprotected areas of the wall, only 4 hours after sunset; their experiment was quite similar to the situation reported here, with the difference that the UAV was flown at dawn, i.e. when the period of time for energy loss from the walls of the agro-industrial building was much longer. Therefore, the temperature differences recorded below the eaves (5.1°C between the hottest and the coldest spots) could be explained by this phenomenon. However, it is obvious that there is also a geometrical thermal bridge along the joint between the wall and the eaves; this kind of thermal bridge is unavoidable and is not related to either defective insulation or poor construction design. Another possible reason for these temperature differences is air leakage from the building to the inner space between the horizontal eaves and the roof slope.

It is important to note that the temperature differences observed below the eaves could be the result of a combination of several phenomena, as explained above, but it is not possible to determine the exact contribution of each one by means of an external qualitative IR survey. Further information could be obtained by carrying out an internal IR survey or by taking photographs from the drone at a shorter distance at different times and at different outdoor temperatures. To analyse this thermal anomaly in more detail, it would be necessary to carry out further in-depth studies, such as contact thermometer measurements to correct apparent temperatures (25), quantitative IR methodologies (26-28), computer simulations (29) or air infiltration tests (30, 31).

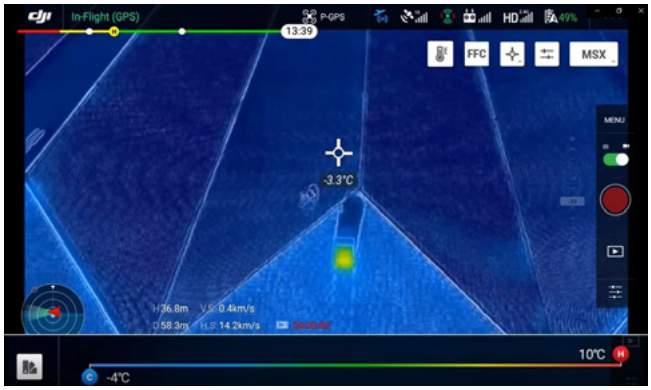

Figure 9. Temperature differences detected by the thermal camera: Flue in the roof.

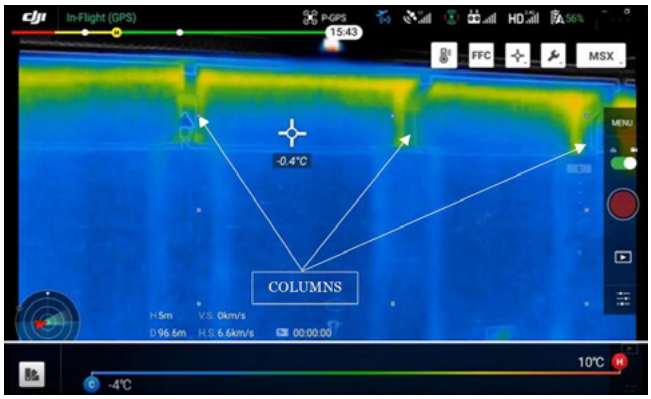

Figure 10. Thermal image of the southwest wall taken during the second inspection flight.

In addition, Figure 10 shows that the upper parts of the concrete columns, which were partially exposed, were warmer than the wall. Since the columns were located between the precast concrete panels, as can be seen in Figure 11, this temperature difference can be explained by the fact that the columns did not have any insulation at all, whereas the concrete panels had a core made of insulation material. Thus, heat could easily flow through the concrete columns. Figure 11 illustrates the heavy insulation (rock wool, air chamber

and brick cladding) that covered the exterior side of the wall panels and also surrounded the columns up to 7.20 m high, as can be seen in Figure 6. However, these insulation layers did not cover the upper parts of the columns because of aesthetic criteria and the need to rest the eaves on the column brackets. Consequently, the thermal anomaly recorded did not indicate a defect in envelope execution, but rather a thermal bridge associated with the design of the structure and envelope system. Considering the volume of the building and the total surface area of its envelope, this thermal anomaly was not considered important. Nevertheless, this information could be employed in future projects to rethink and improve this kind of structures in order to design more energy-efficient buildings.

Another point can be added to the reasons already given above to explain the thermal anomalies shown in Figure 10. The properties of the different construction materials – particularly their emissivity values – influence the quantity of IR radiation emitted. Both the eaves and the columns were made of reinforced concrete, whereas the outside walls consisted of brick cladding. These two materials have different emissivity ratios: 0.94 and 0.90, respectively (32).

In light of the results obtained, the flight plan designed in stage 2 of the protocol proved satisfactory. However, it would be necessary to design a different plan in the case of other buildings or study objectives, since flight plans must be tailored to each specific case. Drone flight planning entails consideration of multiple factors, including distance to target, altitude, flight speed, degree of overlap and flight pattern (8).

The literature contains various recommendations on distances, which vary widely from less than 1 m to detect cracks in concrete or structural elements (33) to 25 m or more for 3D modelling of buildings (34). Hence, it seems clear that there is no ideal distance and this must be established according to the specific objectives of the inspection and the characteristics of the building and its surroundings. Subsequent analysis of the images captured in this study confirmed that the distance established was satisfactory. In the case of a maintenance inspection of an "old" building, a closer distance to the surfaces to inspect would be advisable in order to facilitate detection of cracks, rusting and other damage.

In order to cover the entire area of interest, the most common solution is to fly the drone in horizontal or vertical bands in a zigzag pattern. However, flight paths can also be designed based on other geometric or mathematical optimisation principles (8). In this study, the exterior walls were inspected using the perimeter walk around survey method because the pilot accompanied the drone throughout the flight, scanning the entire height of the cladding in a single flyby (Figure 4). On the contrary, the roof was inspected by flying the drone in a horizontal zigzag pattern with distance of 24 m between the centre of the bands with an overlap of approximately 3 m or 12% (Figure 5): the required number of bands and the overlap between them are obviously related to the visual field of the camera and to the distance between the drone and the object. Recommendations for much higher overlap values, up to 95%, can be found in the literature (35) when the aim of the flight is to create a 3D model of the building based on photographs taken at specific points. In the present work a high overlap was neither necessary nor efficient, since the only purpose of overlapping was to prevent loss of information. Percentage of overlap should be adjusted depending on pilot skills, drone model, distance to target, wind velocity, objectives of the inspection, and so on.

Meanwhile, drone speed is related to the planned flight length and UAV battery life, and camera and drone constraints must also be taken into account to ensure satisfactory capture of photographs/video. These three elements (speed, length and battery) must be considered simultaneously in order to estimate the number of batteries that will be needed. Practical experience suggests that it is always desirable to have a replacement battery available, although calculations could indicate that this is not a priori necessary, and also to define several

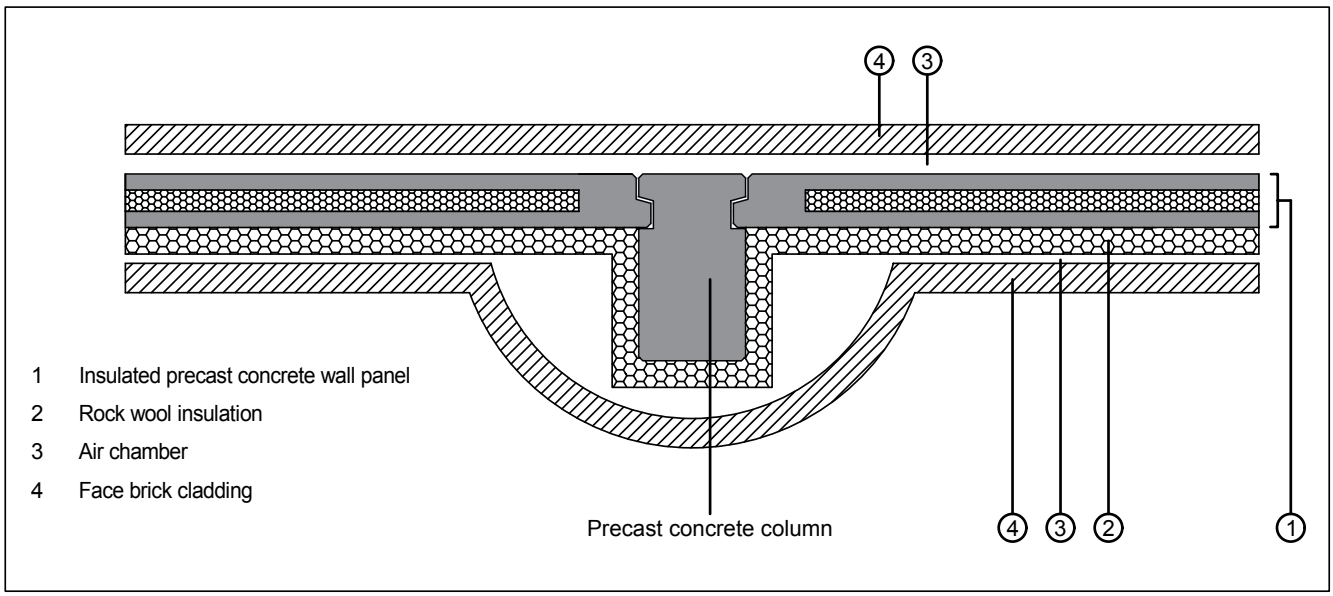

Figure 11. Cross section view of the wall at 1.00 m high

additional landing areas wherever possible. These latter can be used if the drone is unable to reach the initially envisaged landing area because the battery has run out sooner than expected, because of a sudden change in weather conditions or because an unexpected and potentially dangerous element has invaded the drone flight path. Horla and Cieślak studied energy-optimal trajectories for landing of UAVs (36).

In the case study presented here, it was essential to obtain thermal images. Consequently, there were additional factors to consider. It is well known that direct and indirect solar radiation affects the emissivity of materials and can lead to incorrect interpretations, as can humidity, wind or the angle between camera and surface (10). In addition, the type of thermographic camera used here required a difference of at least 10 K (10°C) between internal and external ambient temperature. Hence, the thermal images were captured on a clear day early in the morning before sunrise, at a temperature of 5°C. However, although these conditions were ideal for thermography, they may not be suitable for taking photographs or videos with visible light, since there may be insufficient illumination in some areas of the building envelope. Therefore, as explained earlier, the complete building inspection was conducted by means of two flights at different times. The first inspection, carried out under high illumination at mid-day on a partially clouded day at a temperature of 28°C, obtained pictures of the visible spectrum in optimal visibility and provided initial guidance for the thermographic survey. Subsequently, after analysing the images obtained, the second inspection was planned and executed with the aim of capturing quality thermal images. It is common practice to conduct more than one inspection with a drone and to plan the next flight based on previous inspections, a strategy that some have called the Next-Best-View (NBV) (37). The first flight would also have served to inspect any photovoltaic installation using the IR camera (17).

Image interpretation is the most complex aspect of thermography. As explained before, not all thermal differences apparent in the thermographic images corresponded to problems. Thus, before concluding that thermal differences are due to defects in need of rectification, it is first necessary to take into account the emissivity of the various materials as well as geometric or other details that could distort temperature values (10); the above discussion on the thermal anomalies detected illustrates the difficulties in interpreting images in qualitative IR surveys. However, quantitative analyses fall out of the scope of the present study.

As regards drone operation, the flights demonstrated that guidance was greatly facilitated by the remote controller screen of the DJI Mavic 2 drone, because it made it possible to identify elements in real time. The decision to take a video instead of a series of photographs proved satisfactory: the video was very useful for the engineers involved in construction and commissioning of the building and proved a valuable tool for communication between professionals and with the client.

The IR-UVA inspection did not reveal any relevant defects in envelope execution. However, two thermal anomalies – below the eaves and along the upper part of the columns – were detected and should be followed in time. It is well-known that critical thermal bridges can lead to condensation and mould growth (28).

During the development of the inspection protocol presented here and the subsequent validation flights, various difficulties, precautions and limitations were identified:

- The drone flight may be hindered by the presence of obstacles or other buildings; it is not possible to perform an inspection with a UAV in all cases.
- Nearby buildings owned by other entities, roads or other regulatory constraints may make it necessary to obtain permission from the corresponding air safety agency, with the consequent delays.
- Weather conditions (wind, fog or rain) can prevent execution of a flight or reduce image quality.
- When the goal is to capture thermal images, there must be sufficient difference between the building's interior and exterior temperature and direct solar radiation must also be avoided. Consequently, there will be times of the year when IR-UAV technology will be difficult to implement. It is important to note that the IR camera employed in this study (range of -10°C to 140°C) could be inadequate for cold climates with temperatures under -10°C during extended periods.
- Correct implementation of protocol stages 1, 2 and 3 is fundamental to optimise execution time and drone battery duration.

Although the present study has shown the possibilities offered by IR-UAV systems for the inspection of agro-industrial building envelopes, this tool should be regarded as a complement to other, already established methods. As Vavilov has remarked (38), thermography alone is insufficient to conduct an exhaustive analysis of a building's energy consumption. Moreover, some authors have indicated that thermal bridges are more easily detected from interior surveys with thermographic cameras (39). However, this option is not always possible as it depends on building occupancy and use. In the case of the building studied here, an interior survey will be difficult once the facility is full of barrels, as there will be areas that are impossible to access, underlining the utility of the proposed method.

5. CONCLUSIONS

The present study describes an inspection protocol for agro-industrial buildings using drones. The procedure was validated through application to a real case. The results obtained have demonstrated the capacity of this technology to provide useful information that facilitates building envelope inspection. When combined with thermography, potential thermal anomalies are also detected.

Although UAV and thermography are both well-known technologies, their use in the building sector is not common. Experimentation and the development of standardised methods to serve as guidance would help fill the gap that currently exists in the literature on how to employ IR-UAV technology, its potential and the factors that limit its future use.

The proposed protocol could be used for routine maintenance inspections or energy assessments of not only agro-industrial buildings but also many other types of industrial facility.

6. REFERENCES

(1) Shakhatreh, H., Sawalmeh, A. H., Al-Fuqaha, A., Dou, Z., Almaita, E., Khalil, I., Othman, N. S., Khreishah, A., and Guizani, M. (2019). Unmanned aerial vehicles (UAVs): A survey on civil applications and key research challenges. *IEEE Access*, *7*, 48572-48634. https://doi.org/10.1109/ACCESS.2019.2909530.

(2) Drešček, U., Kosmatin Fras, M., Tekavec, J., and Lisec, A. (2020). Spatial ETL for 3D building modelling based on unmanned aerial vehicle data in semi-urban areas. *Remote Sensing*, *12*(12), 1972. https://doi.org/10.3390/rs12121972.

(3) Kim, S., Kim, S., and Lee, D. E. (2020). Sustainable application of hybrid point cloud and BIM method for tracking construction progress. *Sustainability*, *12*(10), 4106. https://doi.org/10.3390/su12104106.

(4) Martínez-Carricondo, P., Carvajal-Ramírez, F., Yero-Paneque, L., and Agüera-Vega, F. (2020). Combination of nadiral and oblique UAV photogrammetry and HBIM for the virtual reconstruction of cultural heritage. Case study of Cortijo del Fraile in Níjar, Almería (Spain). *Building Research and Information*, *48*(2), 140-159. https://doi.org/10.1080/09613218.2019.1626213.

(5) Chen, K., Reichard, G., and Xu, X. (2019). Opportunities for applying camera-equipped drones towards performance inspections of building facades. In Y. K. Cho, F. Leite, A. Behzadan y C. Wang (Eds.), *Computing in Civil Engineering 2019: Smart Cities, Sustainability and Resilience* (pp. 113-120). Reston, VA, USA: American Society of Civil Engineers. https://doi.org/10.1061/9780784482445.015.

(6) Nnaji, C., and Karakhan, A. A. (2020). Technologies for safety and health management in construction: Current use, implementation benefits and limitations, and adoption barriers. *Journal of Building Engineering*, *29*, 101212. https://doi.org/10.1016/j.jobe.2020.101212.

(7) Davila Delgado, J. M., Oyedele, L., Ajayi, A., Akanbi, L., Akinade, O., Bilal, M., and Owolabi, H. (2019). Robotics and automated systems in construction: Understanding industry-specific challenges for adoption. *Journal of Building Engineering*, *26*, 100868. https://doi.org/10.1016/j.jobe.2019.100868.

(8) Rakha, T., and Gorodetskky, A. (2018). Review of Unmanned Aerial System (UAS) applications in the built environment: Towards automated building inspection procedures using drones. *Automation in Construction*, *93*, 252-264. https://doi.org/10.1016/j.autcon.2018.05.002.

(9) Grosso, R., Mecca, U., Moglia, G., Prizzon, F., and Rebaudengo, M. (2020). Collecting built environment information using UAVs: Time and applicability in building inspection activities. *Sustainability*, *12*(11), 4731. https://doi.org/10.3390/su12114731.

(10) Vollmer, M., and Möllmann, K. P. (2018). Infrared thermal imaging. Fundamentals, research and applications. Weinheim, Germany: Wiley.

(11) Bienvenido-Huertas, D., Rodríguez-Álvaro, R., Moyano, J., Marín, D., and Rico, F. (2019). Estudio comparativo de los métodos para evaluar la transmitancia térmica en cerramientos opacos en el invierno mediterráneo. *Informes de la Construcción*, *71*(554), e288. https://doi.org/10.3989/ic.62542.

(12) Cañas, I., Martín, S., and González, I. (2003). Aplicabilidad de la termografía para la inspección de los edificios rurales: Caso de una comarca española. *Informes de la Construcción*, *55*(488), 21-28. https://doi.org/10.3989/ic.2003.v55.i488.538.

(13) Wicker, M., Alduse, B. P., and Jung, S. (2018). Detection of hidden corrosion in metal roofing shingles utilizing infrared thermography. *Journal of Building Engineering*, *20*, 201-207. https://doi.org/10.1016/j.jobe.2018.07.018.

(14) Eyssautier-Chuine, S., Mouhoubi, K., Reffuveille, F., and Bodnar, J. L. (2020). Thermographic imaging for early detection of biocolonization on buildings. *Building Research and Information, 40,296-310*. https://doi.org/10.1080/09613218.2020.1730740.

(15) Gómez, J., and Tascón, A. (2019). Metodología y aplicación práctica para la inspección de edificios agroindustriales mediante drones. In F. J. García-Ramos and P. Martín-Ramos (Eds.), *Proceedings of the 10th Iberian Agroengineering Congress* (pp. 144-148). Huesca, Spain: Universidad de Zaragoza. http://dx.doi.org/10.26754/uz.978-84-16723-79-9.

(16) Seo, J., Duque, L., and Wacker, J. (2018). Drone-enabled bridge inspection methodology and application. *Automation in Construction*, *94*, 112-126. https://doi.org/10.1016/j.autcon.2018.06.006.

(17) Entrop, A. G., and Vasenev, A. (2017). Infrared drones in the construction industry: designing a protocol for building thermography procedures. *Energy Procedia*, *132*, 63-68. https://doi.org/10.1016/j.egypro.2017.09.636.

(18) Ministerio de la Presidencia y para las Administraciones Territoriales. (2017). Real Decreto 1036/2017, de 15 de diciembre, por el que se regula la utilización civil de las aeronaves pilotadas por control remoto, y se modifican el Real Decreto 552/2014, de 27 de junio, por el que se desarrolla el Reglamento del aire y disposiciones operativas comunes para los servicios y procedimientos de navegación aérea y el Real Decreto 57/2002, de 18 de enero, por el que se aprueba el Reglamento de Circulación Aérea. *Boletín Oficial del Estado*, *BOE 29th December 2017*, *316*. Retrieved from https://www.boe.es/buscar/doc.php?id=BOE-A-2017-15721.

(19) Denominación de Origen Calificada Rioja. Retrieved from https://www.riojawine.com/en/home-en/

(20) Barbaresi, A., De Maria, F., Torreggiani, D., Benni, S., and Tassinari, P. (2015). Performance assessment of thermal simulation approaches of wine storage buildings based on experimental calibration. *Energy and Buildings*, *103*, 307-316. https://doi.org/10.1016/j.enbuild.2015.06.029.

(21) Gómez, J., Tascón, A., and Ayuga, F. (2018). Systematic layout planning of wineries: the case of Rioja region (Spain). *Journal of Agricultural Engineering, 49*(1), 34-41. https://doi.org/10.4081/jae.2018.778.

(22) AENOR-CEN (1998). *UNE-EN 13187 Thermal performance of buildings - Qualitative detection of thermal irregularities in building envelopes - Infrared method (ISO 6781:1983 modified)*. Asociación Española de Normalización (AENOR).

(23) Garrido, I., Lagüela, S., Arias, P., and Balado, J. (2018). Thermal-based analysis for the automatic detection and characterization of thermal bridges in buildings. *Energy and Buildings, 158*, 1358-1367. https://doi.org/10.1016/j.enbuild.2017.11.031.
(24) Kim, C., Choi, J.-S., Jang, H., and Kim, E.-J. (2021). Automatic detection of linear thermal bridges from infrared thermal images using neural network. *Applied Sciences, 11*(3), 931. https://doi.org/10.3390/app11030931.
(25) Ficapal, A., and Mutis, I. (2019). Framework for the detection, diagnosis, and evaluation of thermal bridges using infrared thermography and unmanned aerial vehicles. *Buildings, 9*(8), 179. https://doi.org/10.3390/buildings9080179.
(26) Asdrubali, F., Baldinelli, G., and Bianchi, F. (2012). A quantitative methodology to evaluate thermal bridges in buildings. *Applied Energy, 97*, 365-373. https://doi.org/10.1016/j.apenergy.2011.12.054.
(27) Tejedor, B., Casals, M., Gangolells, M., and Roca, X. (2017). Quantitative internal infrared thermography for determining in-situ thermal behaviour of façades. *Energy and Buildings, 151*, 187-197. https://doi.org/10.1016/j.enbuild.2017.06.040.
(28) Garrido, I., Lagüela, S., Otero, R., and Arias, P. (2020). Thermographic methodologies used in infrastructure inspection: A review—Post-processing procedures. *Applied Energy, 266*, 114857. https://doi.org/10.1016/j.infrared.2020.103481.
(29) Taylor, T., Counsell, J., and Gill, S. (2014). Combining thermography and computer simulation to identify and assess insulation defects in the construction of building façades. *Energy and Buildings, 76*, 130-142. https://doi.org/10.1016/j.enbuild.2014.02.080.
(30) Brinks, P., Kornadt, O., and Oly, R. (2015). Air infiltration assessment for industrial buildings. *Energy and Buildings, 86*, 663-676. https://doi.org/10.1016/j.enbuild.2014.10.040.
(31) Liu, X., Lin, L., Liu, X., Zhang, T., Rong, X., Yang, L, and Xiong, D. (2018). Evaluation of air infiltration in a hub airport terminal: On-site measurement and numerical simulation. *Building and Environment, 143*, 163-177. https://doi.org/10.1016/j.buildenv.2018.07.006.
(32) Quinn Brewster, M. (1992). Thermal Radiative Transfer and Properties. New York, USA: Wiley.
(33) Ellenberg, A., Kontsos, A., Bartoli, I., and Prandhan, A. (2014). Masonry crack detection application of an unmanned aerial vehicle. In Computing in Civil and Building Engineering. In R. Issa Issa and I. Flood (Eds.), *Proceedings of the 2014 International Conference on Computing in Civil and Building Engineering* (pp. 1788-1795). Reston, VA, USA: American Society of Civil Engineers. https://doi.org/10.1061/9780784413616.222.
(34) Zulgafli, M. N., and Tahar, K. N. (2017). Three dimensional curve hall reconstruction using semi-automatic UAV. *ARPN Journal of Engineering and Applied Sciences*, *12*(10), 3228-3232. Retrieved from http://www.arpnjournals.org/jeas/research_papers/rp_2017/jeas_0517_6039.pdf.
(35) Roca, D., Lagüela, S., Díaz-Vilariño, L., Armesto, J., and Arias, P. (2013). Low-cost aerial unit for outdoor inspection of building façades. *Automation in Construction*, *36*, 128-135. https://doi.org/10.1016/j.autcon.2013.08.020.
(36) Horla, D., and Cieślak, J. (2020). On obtaining energy-optimal trajectories for landing of UAVs. *Energies*, *13*(8), 2062. https://doi.org/10.3390/en13082062.
(37) Gupta, R., Barnfield, L., and Gregg, M. (2018). Exploring innovative community and household energy feedback approaches. *Building Research and Information*, *46*(3), 284-299. https://doi.org/10.1080/09613218.2017.1356130.
(38) Vavilov, V. P. (2010). How accurate is the IR thermographic evaluation of heat losses from buildings? *Quantitative InfraRed Thermography Journal*, *7(2)*, 255-258. https://doi.org/10.1080/17686733.2010.9737142.
(39) Fox, M., Coley, D., Goodhew, S., and de Wilde, P. (2014). Thermography methodologies for detecting energy related building defects. *Renewable and Sustainable Energy Reviews*, *40*, 296-310. https://doi.org/10.1016/j.rser.2014.07.188.